frontiers in Earth Science

ORIGINAL RESEARCH
published: 21 February 2022
doi: 10.3389/feart.2022.802052

Correlation of Seismicity With Faults in the South Korea Plateau in the East Sea (Japan Sea) and Seismic Hazard Assessment

Han-Joon Kim[1], Seonghoon Moon[1], Hyeong-Tae Jou[1], Kwang-Hee Kim[2] and Bo Yeon Yi[3]*

[1]Marine Active Fault Research, Korea Institute Off Ocean Science and Technology, Busan, South Korea, [2]Department of Geological Sciences, Pusan National University, Busan, South Korea, [3]Oil and Gas Research Center, Korea Institute of Geoscience and Mineral Resources, Daejon, South Korea

The South Korea Plateau (SKP) is a structural high at the eastern continental margin of the Korean Peninsula. Earthquakes occur frequently in the SKP although they are not larger than M_L 5.0 in magnitude. The SKP is a region of highly rifted continental crust engraved with rifts created during back-arc rifting in the NW Pacific subduction zone that led to the separation of the SW Japan Arc in the Cenozoic. The Bandal, Onnuri, and Okgye Rifts are well-defined rifts in the SKP. Multichannel seismic profiles show that the rifts in the SKP are bounded by large-offset normal faults and their subsided basement is deformed by domino-style faulting. A close spatial correlation is recognized between the epicentral locations of earthquakes with relatively large magnitude and the rift-bounding fault of the Onnuri Rift. The faults in the SKP is interpreted to be reactivated with strike-slip since the middle Miocene. The maximum expected magnitude of earthquakes (Mmax) computed statistically using the catalog including instrumentally recorded seismicity is M_L 5.42. However, Mmax estimated from the catalog including instrumentally recorded seismicity and historical records increases to M_L 6.67.

Keywords: South Korea Plateau, back-arc rifting, active faults, seismic profiles, seismic hazard assessment

OPEN ACCESS

Edited by:
Joanna Faure Walker, University College London, United Kingdom

Reviewed by:
Gianluca Vignaroli, University of Bologna, Italy
Alexis Rigo, Laboratoire de géologie de l'Ecole Normale Supérieure (LG-ENS), France

****Correspondence:***
Han-Joon Kim
hanjkim@kiost.ac.kr

Specialty section:
This article was submitted to Geohazards and Georisks, a section of the journal Frontiers in Earth Science

Received: *26 October 2021*
Accepted: *19 January 2022*
Published: *21 February 2022*

Citation:
Kim H-J, Moon S, Jou H-T, Kim K-H and Yi BY (2022) Correlation of Seismicity With Faults in the South Korea Plateau in the East Sea (Japan Sea) and Seismic Hazard Assessment. Front. Earth Sci. 10:802052. doi: 10.3389/feart.2022.802052

INTRODUCTION

The separation of the SW Japan Arc from (near) the Korean Peninsula proceeded with back-arc rifting and spreading that created the East Sea (Japan Sea), a back-arc sea behind the Japan Arc in the NW Pacific subduction zone (**Figure 1**). The South Korea Plateau (SKP) is a dominant topographic feature at the present continental margin of the middle Korean Peninsula. The SKP is further divided into the eastern and western blocks termed the ESKP and the WSKP, respectively (**Figure 2**). The SKP accommodated extensive fault-controlled crustal deformation associated with back-arc rifting in the early stage of separation of the SW Japan Arc (Kim et al., 2015); as a result, the SKP preserves the fundamental elements of rift architecture consisting of a rift basin (or a trough) rimmed by an uplifted flank.

Earthquakes occur frequently in the SKP, as recorded officially since 1 March 1982 by the Korea Meteorological Administration, although their magnitudes are less than M_L 5.0 (**Figure 2**). However, a noticeable increase in the number of events in recent years is recognized (**Figure 3**). Specifically, the average annual number of events before year 2017 is 1.1; in contrast, the average number since then

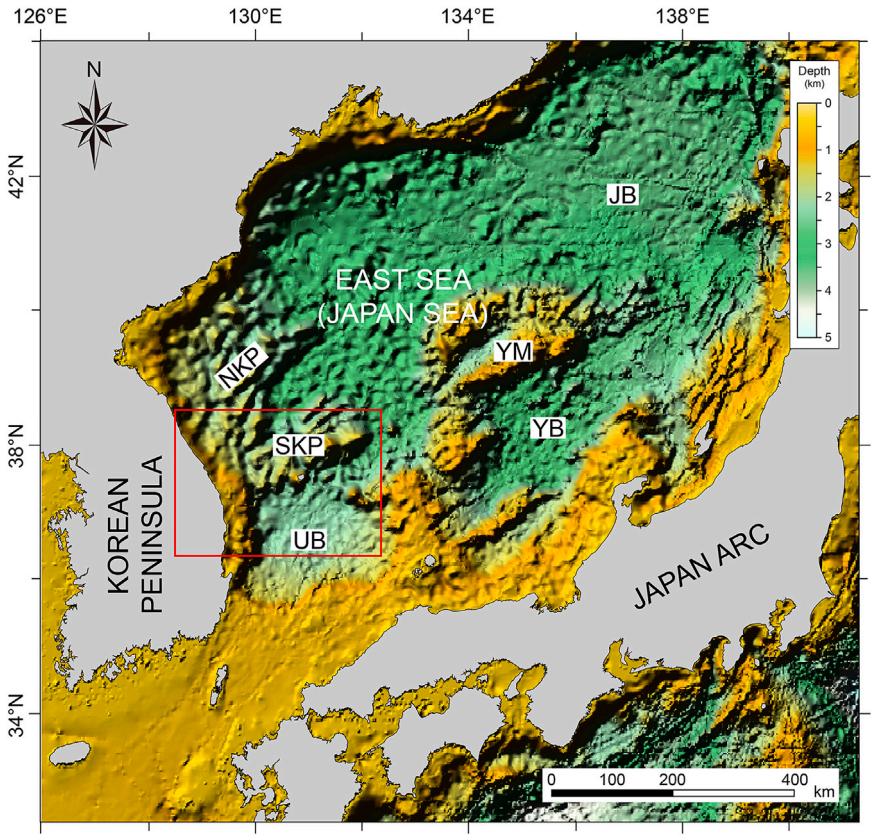

FIGURE 1 | Physiography of the continental margin of the Korean Peninsula in the East Sea (Japan Sea). JB, UB, and YB = Japan, Ulleung, and Yamato Basins, respectively. NKP, SKP, and YM (= North Korea Plateau, South Korea Plateau, and Yamato Bank, respectively) are fragmented continental crust. The red rectangle indicates the study area covering the SKP with detailed bathymetry shown in **Figure 2**.

has increased drastically to 7.8. This increase brought a need to identify active fault structures and assess the seismic hazard potential in the SKP.

The principal objectives of this study are 1) to map faults in the SKP using multichannel seismic (MCS) profiles obtained hitherto, 2) to identify active structures by correlating fault locations with ongoing seismicity, and 3) to estimate the maximum expected magnitude of earthquakes (Mmax) using the statistical method of Kijko et al. (2016). In earlier investigations to address the rifting process in the SKP, (Kim et al. 2007; Kim et al. 2015), identified faults based on a set of MCS profiles. We, in this study, utilize this set of MCS profiles to locate the faults in a more accurate manner. We, then, grouped the faults into rift-bounding faults and the faults within the rifts (i.e., intra-rift faults) to determine active seismic structures that generate the current seismicity.

Tectonic Setting of the SKP

The SKP at the eastern Korean margin is a mass of rifted continental crust segmented into two blocks of the ESKP and the WSKP separated by an about 100 km-long, narrow trough. The WSKP, connected to the Korean Peninsula, about 170 km wide E-W, is composed of several rifts and intervening topographic highs (**Figure 2**). The ESKP takes a trapezoidal shape, measuring about 120 km N-S and 70–110 km E-W. The ESKP is engraved with narrowly-spaced (<20 km), subparallel troughs alternating with ridges aligned NE-SW. These troughs and ridges constitute a system of horsts and grabens. The Bandal, Onnusi, and Okgye Rifts in the WSKP are well-recognized rift structures that are outlined by uplifted rift flanks and bounded by large-offset faults that accommodated major throw downs (**Figure 2**). The central parts of the rifts have depressed bathymetry where fault-controlled subsidence took place dominantly.

Rifting at the continental margin of the Korean Peninsula includes the following processes in Late Oligocene to Early Miocene times (Kim et al., 2015); 1) back-arc rifting and spreading behind the Japan Arc initiated in the northern margin of the Korean Peninsula, resulting in the fragmentation of the Korea Plateau (KP) from the peninsula and the opening of the Japan Basin (**Figure 4A**); 2) while back-arc spreading widened the Japan Basin, back-arc rifting occurred in the middle part of the margin of the Korean Peninsula that eventually developed into breakup and back-arc spreading behind the SW Japan Arc (**Figure 4B**). In this stage southwestward extension propagated from seafloor spreading in the Japan Basin burrowed into the WSKP to induce rifting of the Bandal Rift toward the SE direction. Kim et al. (2015)

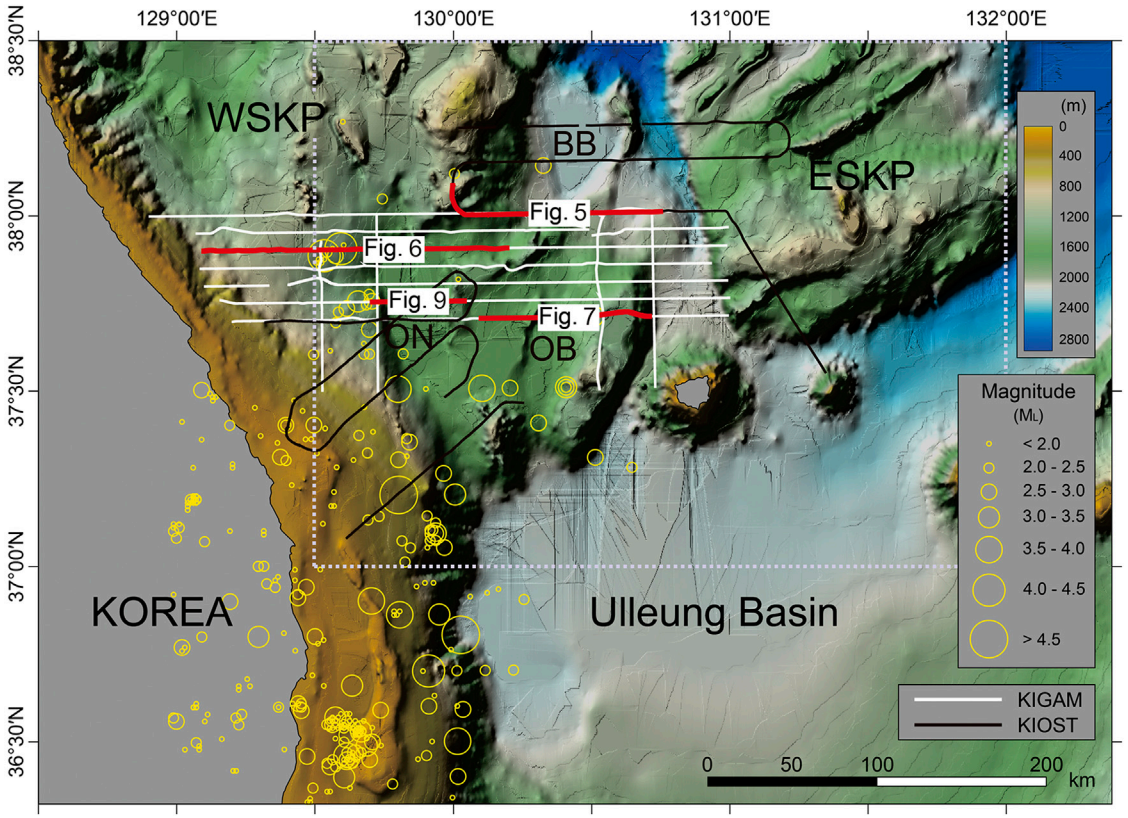

FIGURE 2 | Detailed bathymetry of the SKP overlain with the epicenters of earthquakes instrumentally recorded by the Korea Meteorological Administration (KMA) from 1982 to 2020. The black and white tracks are reflection seismic lines shot by the Korea Institute of Ocean Science and Technology (KIOST) and the Korea Institute of Geoscience and Mineral Resources (KIGAM), respectively. The locations of seismic profile sections that are referred to in the text are highlighted as thick red lines and labeled with a figure number. The dotted rectangle indicates the area for estimating the maximum expected magnitude of earthquakes (Mmax) in this study.

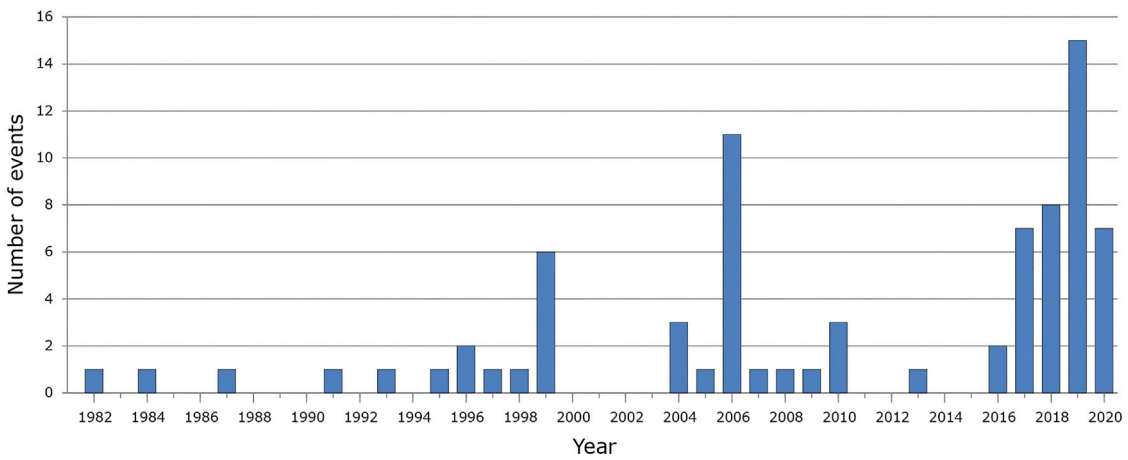

FIGURE 3 | Annual number of seismic events larger than M_L 0.8 at the SKP from 1982 to 2020. The events were recorded by the KMA.

suggested that the SKP underwent maximum extension of continental crust facilitated by depth-dependent stretching.

The Ulleung Basin is a thickly sedimented basin lying further seaward south of the continental slope of the SKP. (Kim et al., 2003; Kim et al., 2015), based on crustal structure from deep seismic sounding data, suggested that the Ulleung Basin is underlain by back-arc oceanic crust that is 2,3 km thicker than normal oceanic crust. They further suggested that 1) the thicker

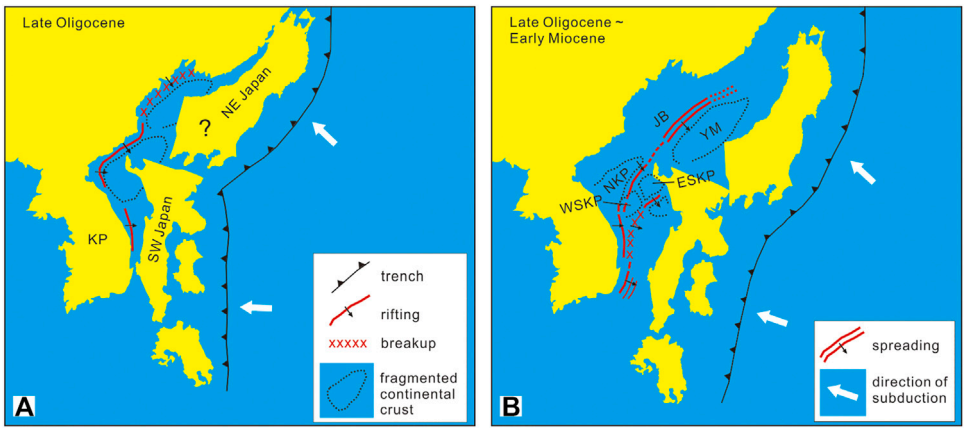

FIGURE 4 | Schematic diagrams showing the processes of back-arc rifting to breakup at the eastern Korean margin associated with the separation of the SW Japan Arc (modified from Kim et al., 2018). **(A)** Initiation of back-arc rifting and breakup at the northern Korean margin. **(B)** Back-arc rifting and breakup at the eastern Korean margin.

than normal oceanic crust underlying the Ulleung Basin was created above the hotter than normal mantle, 2) the SKP, located between the continental crust of the Korean Peninsula and the back-arc oceanic crust under the Ulleung Basin, marks the seaward limit of continental crust rifted with maximum extension, and 3) the slope base of the SKP is the site of breakup that initiated the emplacement of oceanic crust in the Ulleung Basin. In other words, the SKP represents transitional crust between the continental crust of the Korean Peninsula and the back-arc oceanic crust underlying the Ulleung Basin.

The occurrence of earthquakes shows a contrast between the SKP and the Ulleung Basin. Earthquakes occur preferentially in the SKP but rarely in the Ulleung Basin (**Figure 2**), which appears to demarcate the rifted continental crust of the SKP and the back-arc oceanic crust under the Ulleung Basin. The focal depths of the earthquakes in and around the Korean Peninsula average to ~10 km, mostly not exceeding 15 km (Sheen, 2015). However, earthquakes in the SKP occur frequently at the depth range from 15 to over 25 km (Korea Meteorological Administration (KMA) at http://www.weather.go.kr/weather/earthquakevolcano/report.jsp). Kim et al. (2015) inferred the crustal structure of the SKP that indicates the upper and lower crustal boundary at ~15 km depth. Therefore, it seems that earthquakes occur frequently at the lower crustal level. Explanations have been proposed for earthquakes in the lower continental crust such as 1) localized stress amplification in dry materials (e.g., Menegon et al., 2021), 2) faulting in the lower crust in a delamination model for rifting (Lister et al., 1986), and 3) the presence of a brittle-ductile transition in the upper part of the lower crust that sustains rigidity. However, accurate explanations for the deep crustal earthquakes are still in debate.

METHODS AND MATERIALS

The MCS profile sets used in this study include 1) approximately 800 km of 14- or 48-fold migrated seismic profiles from seismic data obtained by the Korea Institute of Ocean Science and Technology (KIOST) and 2) over 1,400 km of 40-fold stacked seismic profiles provided by the Korea Institute of Geoscience and Mineral Resources (KIGAM) (**Figure 3**). The KIOST data were obtained using a 56- or 96-channel streamer that recorded shots from a 1,380 or 690 in^3 air gun array. Processing of the KIOST data included stacking, predictive deconvolution, and 45° finite-difference time migration. The KIGAM data were obtained using an 80-channel streamer and a 924 or 1,254 in^3 air gun array. Processing of the KIGAM data included procedures from trace editing to stacking.

For computing Mmax, we used the magnitude record of the earthquakes in the SKP recorded by the KMA on the local scale (M_L). The earthquake catalog spans the period from 1982 to 2021 and covers the region from 37° to 38.5°N and from 129.5° to 132.0°E that encompasses the WSKP and the ESKP (**Figure 2**). 77 events were recorded with magnitudes ranging from M_L 0.8 to 4.7. However, the earthquakes were azimuthally not well covered by the seismic stations in the Republic of Korea, because 1) the number of seismic stations was not large before year 2000 and 2) most of the seismic stations are located in the southern Korean Peninsula west of the SKP. As a result, we were unable to compute accurate focal mechanism solutions to explain the fault activity.

RESULTS

Faults in the SKP

The faults displacing the basement in the SKP are identified on seismic profiles (**Figures 5**–**7**). We categorize the faults into the rift-bounding and intra-rift faults that occur along the boundaries of rifts and within the rifts, respectively (**Figure 8**). The faults bounding the grabens in the ESKP are considered as rift-bounding faults. Faults identified between the Korean Peninsula and the Onnuri Rift are not categorized as either rift-bounding or intra-rift faults because they occur outside the rifts.

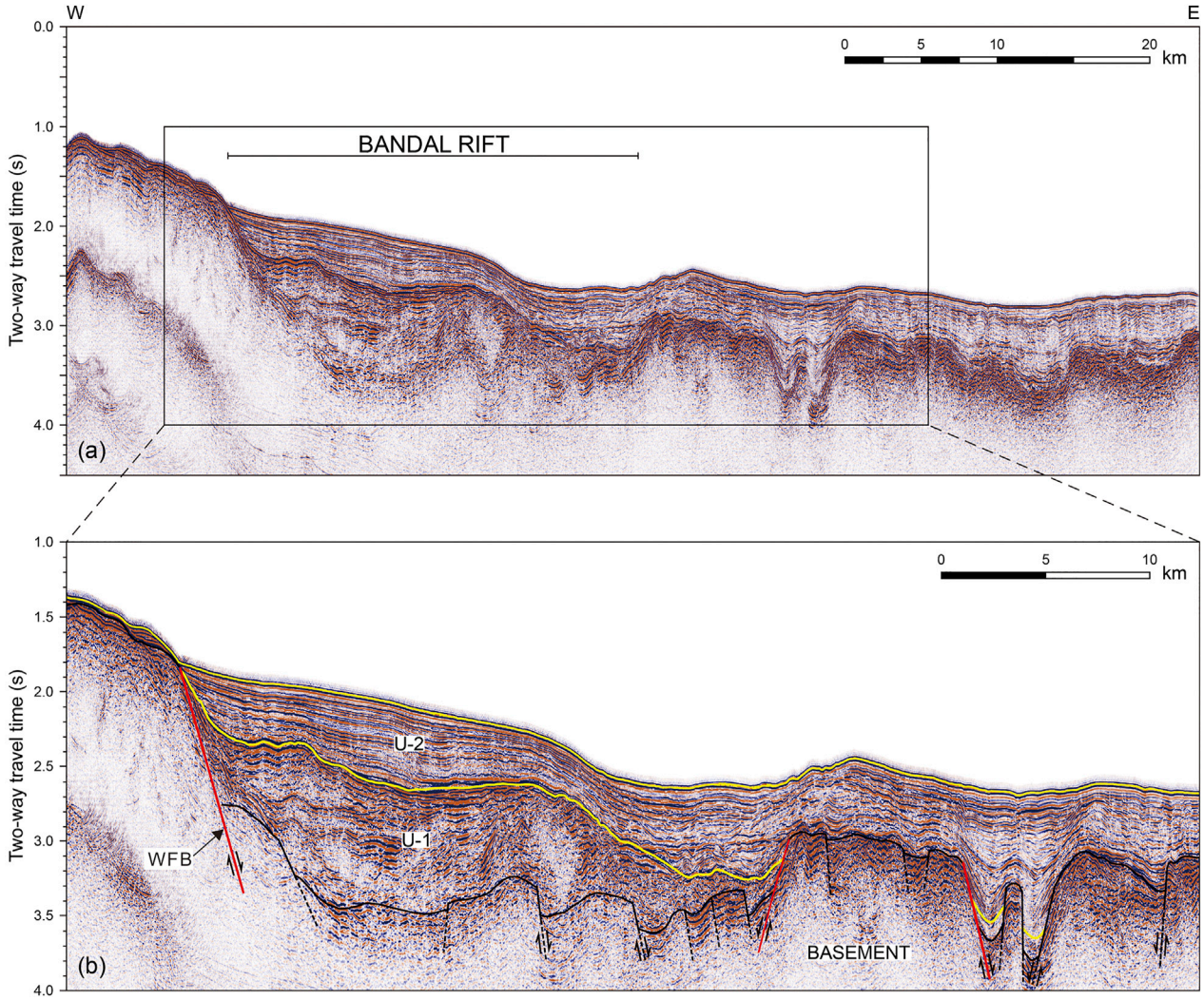

FIGURE 5 | (A) Seismic profile showing the structure of the Bandal Rift (see **Figure 2** for location) and **(B)** its interpretive line drawings. The rift-bounding fault is depicted in red. WFB = western bounding fault of the Bandan Rift. U-1 and U-2 = syn-rift and post-rift sedimentary units, respectively.

Rift-Bounding Faults

For individual rifts in the WSKP, the rift-bounding faults consists of one (or more) fault(s) and occur along the cliff of an uplifted flank that is arcuate outward (**Figures 5**–**8**). Although the spacing of MCS lines seems too large to unequivocally constrain the fault trace and geometry, the faults bounding the rifts are well recognized and traced on MCS profiles in conjunction with bathymetric data. The rift-bounding faults created first-order subsidence of the basement with a major throw down expected by extensional rifting (**Figures 5**–**7**).

Overall, the rifts in the WSKP show an asymmetric profile with the hanging wall tilted down toward the major rift-bounding fault zone on one side that accommodated a large throw down. The Okgye Rift is typical of a half-graben bounded by a large-offset fault on one side (**Figure 7**). The Bandal and Onnuri Rifts are bounded by a large-offset fault zone on one side and a subsidiary fault zone on the opposing side with much smaller offset (**Figures 5**, **6**). Specifically, the bounding fault of the Onnuri Rift on the eastern side (fault "EFO" in **Figure 6**) is well recognized that induced a large vertical displacement. In contrast, the western bounding fault of the Onnuri Rift is difficult to identify because 1) a large-offset fault antithetic to the EFO is not readily recognized in the western border fault zone and 2) the western flank of the Onnuri Rift is broad and highly deformed by faults (**Figure 6**), causing local depressions of the basement rocks. However, we interpret fault WFO (**Figure 6**) as the western bounding fault of the Onnuri Rift because it is antithetic to fault EFO and bounds the intra-rift zone deformed by domino-style faulting which will be explained later in "2) Intra-rift faults". Continental rifting includes formation of a half-graben tilted down toward a large-offset fault zone (e.g., Rosendahl et al., 1986). In a more advanced stage, a half-graben develops into a full-graben with an antithetic fault zone on the opposing side. Therefore, it appears that the

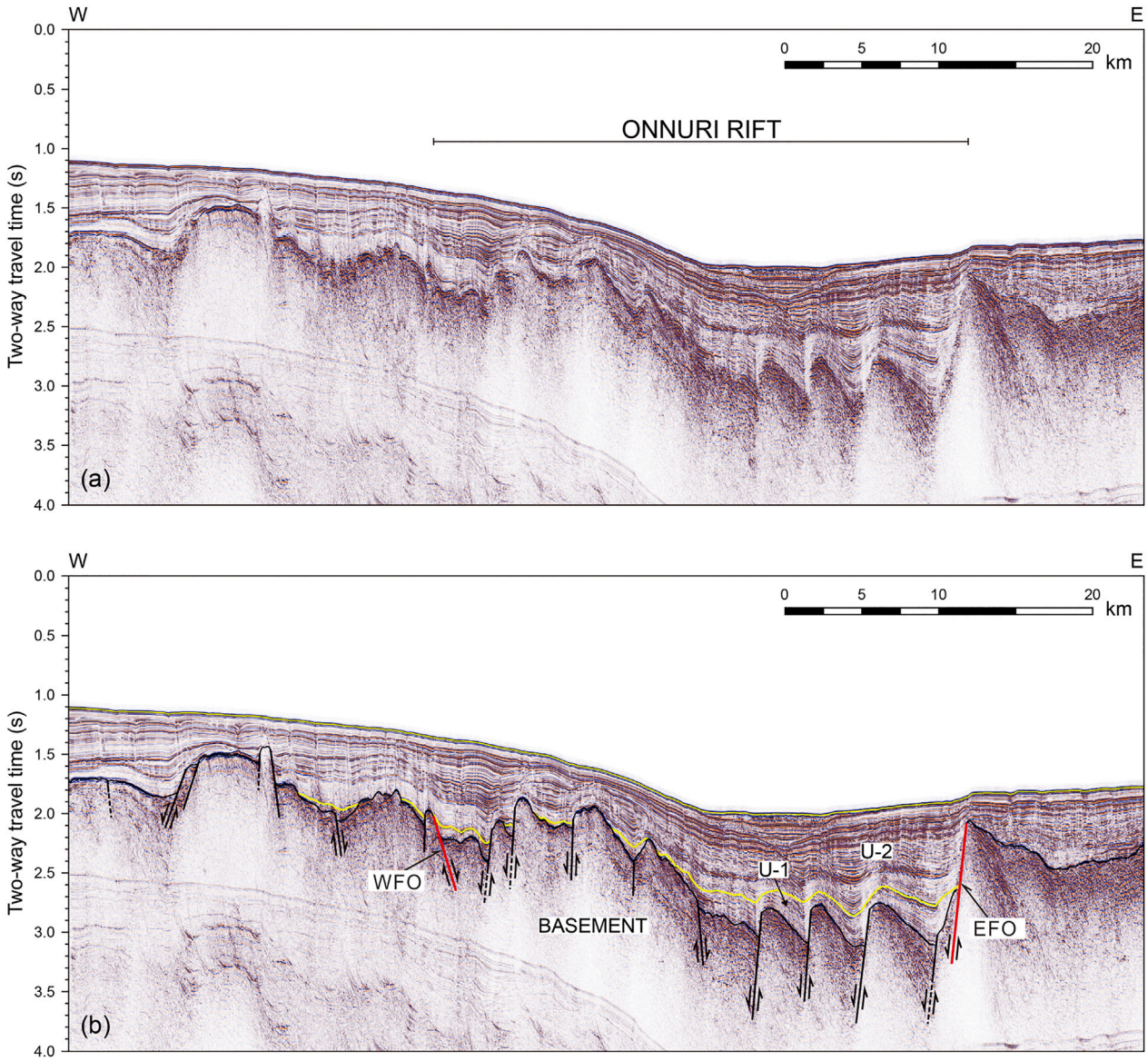

FIGURE 6 | (A) Seismic profile showing the structure of the Onnuri Rift (see **Figure 2** for location) and **(B)** its interpretive line drawings. Note that the basement of the Onnuri Rift is deformed by domino-style normal faulting between the eastern and antithetic western bounding faults, EFO and WFO, respectively (see the text). The rift-bounding fault is depicted in red. U-1 and U-2 = syn-rift and post-rift sedimentary units, respectively.

Bandal and Onnuri Rifts underwent a more advanced stage of rifting.

The orientation of the rift-bounding faults is perpendicular to the direction of extension induced by initial rifting. If we assume that extension occurred seaward, rifting occurred to the SE direction in the Bandal Rift, eastward in the Onnuri Rift, and dominantly eastward in the Okgye Rift. The uplifted flank occurring along the SE boundary of the Bandal Rift is well recognized on the bathymetry map (**Figure 8**), extending southwestward to the N-S trending eastern boundary fault of the Onnuri Rift; it also cuts the N-S trending intra-rift faults in the Okgye Rift. In other words, the uplifted flank of the Bandal Rift overprinted the NS-trending structures of the Okgye Rifts, suggesting that rifting in the Bandal Rift persisted after the initiation of rifting in the Okgye Rift.

Intra-Rift Faults

The central part of the rifts bounded by rift-bounding faults shows depressed bathymetry where prominent subsidence and deposition of thick sediments took place. The depression is clearly recognized in the Bandal and Onnuri Rifts, whereas it is less clear in the Okgye Rift. The subsided acoustic basement in the rifts is dissected by numerous intra-rift faults. In the Onnuri and Okgye Rifts, the intra-rift faults created basement highs alternating with lows (**Figures 6**, **7**). Here, back-tilting of the surface of a fault block between two consecutive faults is recognized, being representative

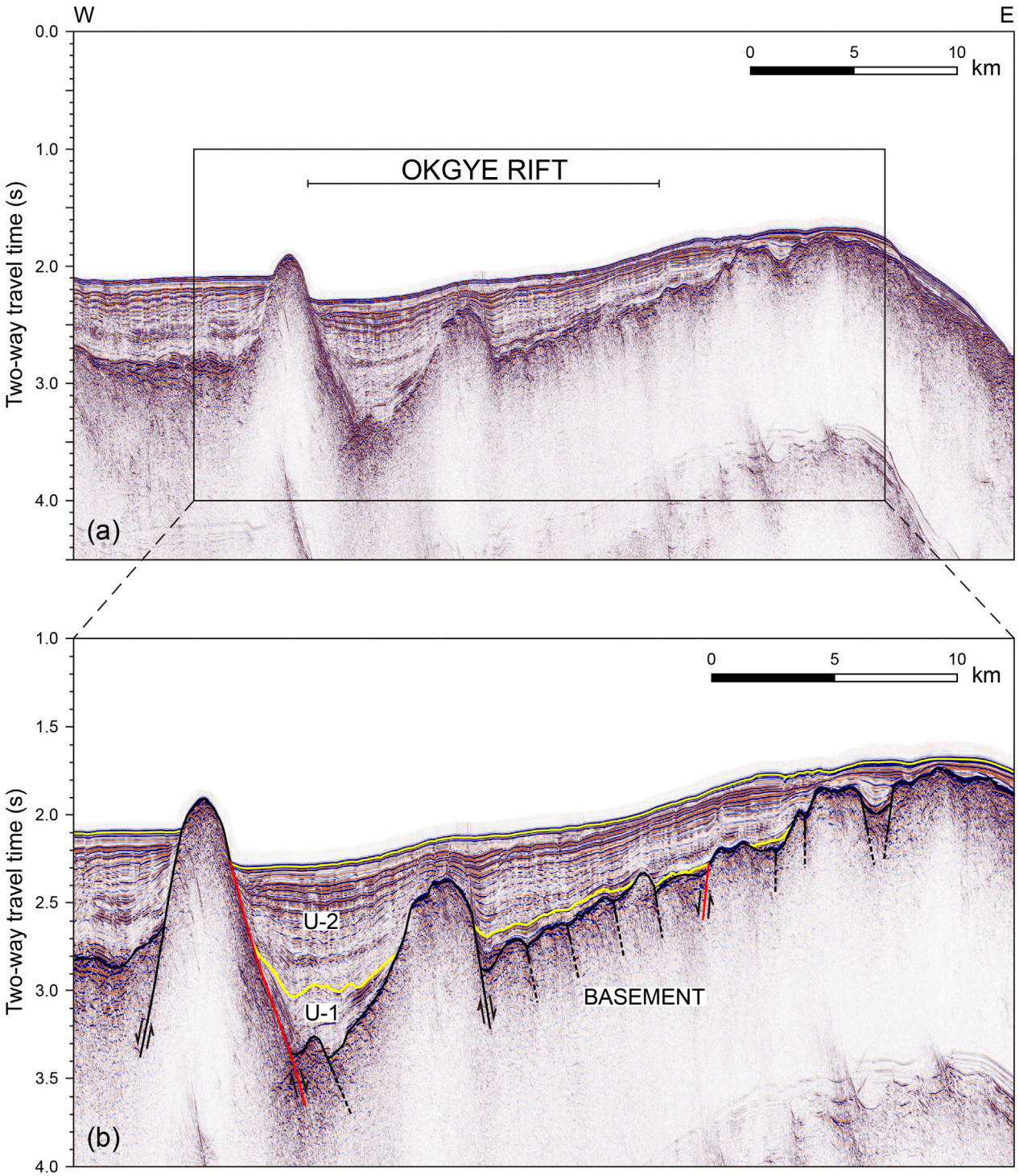

FIGURE 7 | (A) Seismic profile showing the structure of the Okgye Rift (see **Figure 2** for location) and **(B)** its interpretive line drawings. The rift-bounding fault is depicted in red. U-1 and U-2 = syn-rift and post-rift sedimentary units, respectively.

of domino-style normal faults (Kim et al., 2015). The domino faults are well traced in the Onnuri Rift; the domino faults tend to be evenly spaced and subparallel to the rift-bounding fault. The central part of the Onnuri Rift that is wider than other parts between two rift-bounding faults (**Figure 8**) is interpreted to have experienced a higher degree of extension.

In the Bandal Rift, domino-fault structure showing back-tilting of the surface of a fault block is not so explicitly

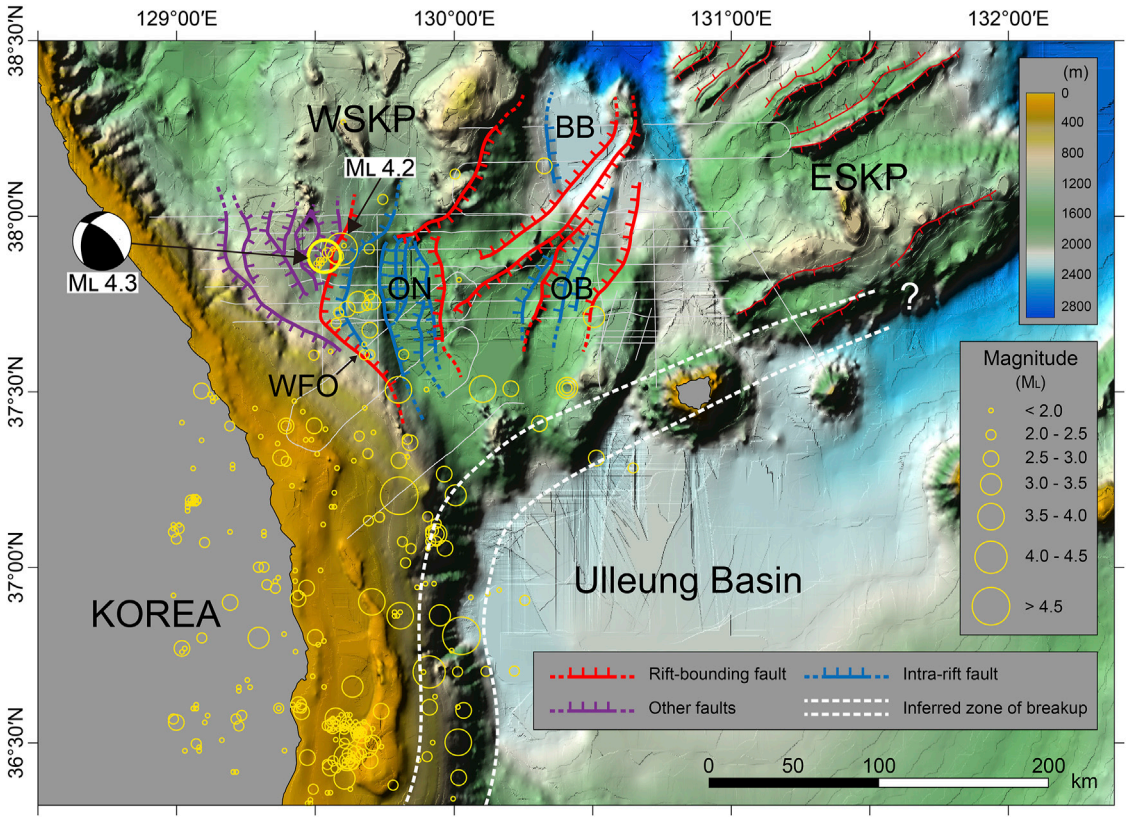

FIGURE 8 | Geologic structural map of the South Korea Plateau overlain with the epicenters of earthquakes. WFO, Western bounding fault of the Onnuri Rift.

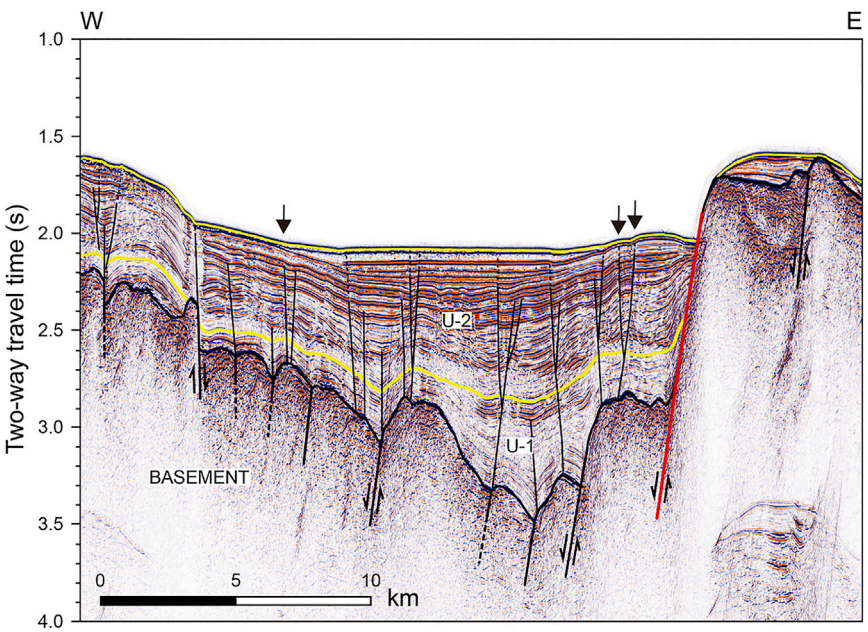

FIGURE 9 | Seismic profile showing sedimentary structure above the acoustic basement in the Onnuri Rift (see **Figure 2** for location). The arrows indicate faults that enable the recognition of increasing vertical separations of the sedimentary layers with depth in post-rift unit U-2.

TABLE 1 | Maximum magnitude of earthquakes (Mmax) expected at the SKP and their return period (RP) computed by the HA3 software (Kijko et al., 2016).

Procedures	[1)]Mmax (M_L)/RP (yr.) (B-value)	[2)]Mmax (M_L)/RP (yr.) (B-value)
Maximum likelihood	4.86 ± 0.25/370 (0.63 ± 0.10)	6.59 ± 0.40/1920 (0.66 ± 0.07)
Gibowicz-Kijko	6.07 ± 1.40/1,680 (0.67 ± 0.09)	6.52 ± 0.24/124 (0.74 ± 0.06)
Gibowicz-Kijko-Bayes	5.63 ± 0.95/2,250 (0.66 ± 0.09)	6.61 ± 0.39/1860 (0.66 ± 0.07)
Kijko-Sellevoll	5.49 ± 0.81/600 (0.65 ± 0.09)	6.92 ± 0.67/1,370 (0.66 ± 0.07)
Kijko-Sellevoll-Bayes	5.26 ± 0.59/670 (0.65 ± 0.09)	6.54 ± 0.33/4,150 (0.65 ± 0.07)
Tate-Pisarenko	Failed	Failed
Tate-Pisarenko-Bayes	Failed	6.71 ± 0.47/2,120 (0.66 ± 0.07)
Non-parametric (Gaussian)	5.18 ± 0.52/440 (0.65 ± 0.09)	6.82 ± 0.58/1,210 (0.66 ± 0.07)
Average	5.42 ± 0.75/1,002 (0.65 ± 0.09)	6.67 ± 0.44/1980 (0.67 ± 0.07)

[1)]The catalog includes instrumentally recorded events.
[2)]The catalog includes instrumentally recorded events and historical events.

recognized as in the Onnuri Rift. However, intra-rift faults toward the western major bounding fault in the Bandal Rift ("WFB" in **Figure 5**) appears to be sub-parallel and dipping in the similar direction, suggesting a certain component of domino faulting. We note that we traced a limited number of the intra-rift faults that appear to be traced continuously over consecutive profiles, although the basement is deformed by abundant faults.

Faults in Sediments

The rifts in the WSKP are filled with well-stratified sedimentary sequences that consist of underlying syn-rift (U-1) and overlying post-rift (U-2) units (**Figures 5–7**). Kim et al. (2015) inferred the age of U-1 to be Late Oligocene to Early Miocene, which is consistent with paleontological age dating of sediments by Tsoy et al. (2017) and the subsidence curves at the southern part of the eastern Korean margin derived by Ingle. (1992). The U-1 unit takes an overall wedge form across the rifts, placing the thick end on a major large-offset rift bounding fault. The wedge form implies tilting of the hanging wall during deposition. The thickening of U-1 is also recognized toward the individual hanging wall of domino faults. In addition, the syn-rift unit is uplifted alternatingly above the tilted basement highs. These features indicate that domino-style faulting persisted during the deposition of U-1.

Overall, the overlying post-rift unit, U-2, consists of parallel reflections, which suggests insignificant tectonic activities during its deposition. Numerous faults are identified within the sediments that extend to the uppermost sequences or to the seafloor (**Figure 9**). These faults occur not only across the subsided hanging wall blocks but also in the uplifted footwall blocks, implying diffuse deformation in the SKP by the current stress field. In many places, the faults developed into branching splays spreading upward (**Figure 9**), representative of a flower structure created by strike-slip faulting. The flower structures are recognized noticeably in the U-2 unit.

Although faults in the post-rift unit, U-2, are noticeable, vertical displacement of sedimentary sequences caused by faulting is small or not readily recognized. As the main reason, strike-slip faulting did not cause large vertical displacement of post-rift sediments that were deposited horizontally. As another reason, small vertical displacement is not resolved on seismic profiles obtained using an air-gun source. Nevertheless, an increase in vertical displacement with depth caused by faulting in the U-2 unit is recognized along some faults (**Figure 9**), which indicates faulting took place coevally with the deposition of the sequences. If faulting had occurred as a single event after deposition, the sequences cut by the faults would have equal vertical displacement. We, therefore, interpret that strike-slip faulting has been a dominant mode of deformation in the SKP since the middle Miocene.

DISCUSSION

Analysis of Seismic Hazards in the SKP

Correlation of Faults With Seismicity

All the recorded earthquakes have occurred in the WSKP (**Figure 8**); in contrast, earthquakes in the ESKP have not been recorded. In the WSKP, earthquakes have small-to-medium magnitude not exceeding. Only two earthquakes (M_L 4.3 and 4.2) occurred with magnitude larger than M_L 4.0 in the WSKP north of 37°30′N where rifts are identified on seismic profiles. The majority of earthquakes in the SKP occurs on or close to the WFO in the western part of the Onnuri Rift (**Figure 8**), suggesting a spatial correlation between the epicentral locations and rift structures. In contrast, the abundant rift-bounding and intra-rift faults elsewhere in the SKP generate much less earthquakes, although seismic profiles show intra-rift faults extend upward to the seafloor. In particular, the WFO appears to be a prominent active structure with more concentrated seismicity than others; seismicity here includes all of the two relatively large earthquakes with magnitude greater than M_L 4.0. The WFO appears to extend southeastward toward the inferred zone of breakup along the base of the continental slope at the eastern continental margin the Korean Peninsula (**Figure 8**), marking the site of the majority of seismic events at the entire Korean margin in magnitude as well as in number.

Extension at the eastern Korean margin during back-arc rifting and spreading ceased in the middle Miocene (around 14–15 Ma), then, the margin became subjected to compression in the NNW-SSE (or N-S) direction (e.g., Lee et al., 2011). The compressional stress changed its direction again to ENE-WSW

TABLE 2 | Historical earthquake record from A.D. 2 to 1904 (Kyung, 2012).

Date (year. month. day)	Intensity (I)	[1)]Magnitude (M_L)
1,511. 03. 21	IV	3.98
1,521.10. 12	IV	3.98
1,522. 01. 19	IV	3.98
1,526. 04. 01	IV	3.98
1,546. 12.16	III	3.41
1,558. 12. 09	IV	3.98
1,681. 06.21	VIII	6.28
1,681. 06. 27	VIII	6.28
1,681. 12. 20	VI	5.12

[1)]*Equation for conversion from intensity (I) to magnitude (ML) is ML, 1.7 + 0.57 I (Kim and Kyung, 2015).*

since the Pliocene. The ENE-WSW compression has persisted to the present, as indicated by focal mechanism solutions of earthquakes in and around the Korean Peninsula (Rhie and Kim, 2010). These directions of compressive stress since the middle Miocene are different from the direction of extension during back-arc rifting. The WFO and its adjacent faults that are inferred to be active structures are orientated dominantly N-S or NW-SE (**Figure 8**), which is oblique to the directions of compression since the middle Miocene. We. therefore, interpret that the active structures in the SKP have been reactivated with a strike (or oblique) slip component.

The largest earthquake ever recorded in the SKP is the M_L 4.3 event that occurred recently on April 19, 2019. The focal mechanism solution of this event is available from the International Seismological Center (ISC) and the National Research Institute for Earth Science and Disaster Resilience (NIED). The focal mechanism solution indicates with reverse slip with a strike-slip component with strike = 194° (or 316°), dip = 34° (or 70°), and rake = 142° (or 62°) (**Figure 8**). Our interpretation appears to be in agreement with the focal mechanism solution.

Assessment of Seismic Hazards in the SKP

The potential maximum magnitude of earthquakes (Mmax) expected on a fault can be estimated using the length of the fault (e.g., Anderson et al., 1996). However, it is difficult to define the coseismic segments of faults in the SKP based on seismic profiles because the faults, rift-bounding and intra-rift, do not consist of straight portions; instead, they have arcuate or curvilinear traces. Non-straight faults cause a scatter in the relationship between the maximum throw and the surface rupture length (Iezzi et al., 2018, 2020), making it difficult to estimate Mmax using the fault length. In addition, large earthquakes with aftershocks have not occurred that enable us to trace the length of coseismic source structures.

In this study, Mmax in the SKP and their return period (RP) were estimated statistically using the software, HA3 (Kijko et al., 2016), suited for a specific area based on the catalog of instrumentally recorded events and historical records. The seismicity catalog for HA3 includes 56 events recorded since 1 March 1982 that are larger than M_L 2.0, a threshold magnitude for computation. Six statistical procedures were performed successfully by HA3 (**Table 1**). Mmax ranges from M_L 4.86 to M_L 6.07, averaging to M_L 5.42 with the return period of 1,000 years, suggesting that the potential seismic hazard is not high in the SKP.

The b-value in the Korean Peninsula computed from the instrumental earthquake catalog is 1.11 (Noh et al., 2000), which is higher than the b-value at the entire continental margin of the Korean Peninsula ranging from 0.85 to 0.88 (Hong et al., 2020). The b-value in the SKP from the instrumental catalog ranges from 0.63 to 0.67, averaging to 0.62 (**Table 1**), which is noticeably lower than the b-values in the Korean Peninsula and its entire continental margin. The low-to-intermediate b-values may suggest the dominance of relatively large earthquakes over smaller earthquakes (e.g., Wu et al., 2018).

Although the magnitude of instrumentally recorded earthquakes is not large, the historical record from A.D. 2 to 1904 compiled by the Korea Meteorological Administration (2012) indicates occurrences of 10 earthquakes with relatively large intensities felt in the coastal area north of 37°N (**Table 2**) that were interpreted to have occurred in the coastal and offshore region encompassing the SKP. The intensities of those earthquakes are mostly larger than or equal to IV. Two of them had remarkably large intensity of VIII. The intensity of the historical events can be converted to the M_L magnitude using the relation proposed by Kim and Kyung (2015) (**Table 2**). Conversion suggests the M_L magnitude of the two historical events in 1,681 is as large as 6.28. Including historical earthquakes in the catalog resulted in average Mmax of M_L 6.67 with the return period of 1980 years (**Table 1**). Therefore, we find that 1) the long-term Mmax value is significantly larger than that estimated from the current seismicity and 2) the hazard potential of the long-term Mmax is not high, considering its return period of about 2000 years. The historical record includes four events larger than M_L 4.0 for about 500 years since 1,511, whereas instrumental record includes three events larger than M_L 4.0 for less than 40 years since 1982. Therefore, we note that the historical record may be subjected to incompleteness, considering offshore earthquakes were difficult to be felt on land unless their magnitudes were large enough.

As mentioned previously, the basement blocks in the rifts in the SKP are tilted toward the rift-bounding faults and deformed by abundant domino-style normal faulting. Tilting of the hanging wall during rifting is frequently caused by slip on the listric normal fault (e.g., McClay, 1990). Back-tilting of domino-fault blocks is facilitated by slip on the lower flatter portion of a listric normal faults below (e.g., McCann and Saintot, 2003). Therefore, the rift bounding faults in the SKP are interpreted to have been created as listric normal faults. Wu et al. (2018) suggested that the thrust faulting regions have lower b-values than normal faulting regions. The lower, flatter portions of listric fault planes are easily reactivated as thrusts, whereas reactivation of the higher steeper portions as reverse faults is mechanically more difficult (Jain et al., 2013). Therefore, the low b-values in the SKP may indicate the dominance of thrust faulting on the lower flatter portions of the rift-bounding faults and intra-rift faults.

CONCLUSION

The South Korea Plateau (SKP) preserves fault-controlled rift structures associated with back-arc rifting in the

Cenozoic. We identified faults in the SKP and correlated them with ongoing seismicity. The results of our study are as follows:

1 The deformation of the SKP during back-arc rifting is explained by normal faulting along the rift boundaries and domino-style extensional faulting within the rifts.
2 The deformation of the post-rift sequences suggests the reactivation of the faults as strike-slip faults under the current compressive stress.
3 All the recorded earthquakes have occurred in the western block of the SKP. The western bounding fault zone of the Onnuri Rift is a prominent active structure with concentrated seismicity with relatively large magnitude.
4 The maximum possible magnitude of earthquakes (Mmax) in the SKP, estimated statistically from the instrumental seismicity catalog is M_L 5.42 on average with the return period of 1,000 years. Mmax estimated from the catalog including both instrumentally recorded and historical earthquakes increases to M_L 6.67 with the return period of 2000 years.
5 The average b-value of .65 in the SKP is lower than that in the Korean Peninsula, which may suggest the dominance of thrust faulting on the listric rift-bounding faults.

DATA AVAILABILITY STATEMENT

The raw data supporting the conclusion of this article will be made available by the authors, without undue reservation.

AUTHOR CONTRIBUTIONS

H-JK: conception, design, and writing of the work. SM: interpretation of seismic data. H-TJ, K-HK and BY: acquisition and processing of seismic and earthquake data.

FUNDING

This work was funded by the Korea Institute of Ocean Science and Technology (Grant PE99941), the Korea Meteorological Administration (Grant KMI 2018-02810-4), and the Ministry of Oceans, and Fisheries of Korea (Grant PG55261).

ACKNOWLEDGMENTS

H-JK thanks Dr. A. Kijko for providing the HA3 software. He appreciates Dr. J. Faure Walker and reviewers for constructive comments.

REFERENCES

Anderson, J. G., Wesnousky, S. G., and Stirling, M. W. (1996). Earthquake Size as a Function of Fault Slip Rate. *Bull. Seismol. Soc. Am.* 86, 638–690.

Hong, T.-K., Park, S., Lee, J., and Kim, W. (2020). Spatiotemporal Seismicity Evolution and Seismic hazard Potentials in the Western East Sea (Sea of Japan). *Pure Appl. Geophys.* 177, 3761–3774. doi:10.1007/s00024-020-02479-z

Iezzi, F., Mildon, Z., Walker, J. F., Roberts, G., Goodall, H., Wilkinson, M., et al. (2018). Coseismic Throw Variation across Along-Strike Bends on Active Normal Faults: Implications for Displacement Versus Length Scaling of Earthquake Ruptures. *J. Geophys. Res. Solid Earth* 123, 9817–9841. doi:10.1029/2018JB016732

Iezzi, F., Roberts, G., and Faure Walker, J. (2020). Throw-rate Variations within Linkage Zones during the Growth of normal Faults: Case Studies from the Western Volcanic Zone, Iceland. *J. Struct. Geology.* 133, 103976. doi:10.1016/j.jsg.2020.103976

Ingle, J. C., Jr. (1992). "Subsidence Pattern of the Japan Sea: Stratigraphic Evidence from ODP Sites and Onshore Sections," in *Pro. ODP Sci. Res.* Editors K. Tamaki, K. Suyehiro, J. Allan, and M. McWilliams, 127/128, 1197–1218.

Jain, A., Verma, A. K., Vishal, V., and Singh, T. N. (2013). Numerical Simulation of Fault Reactivation Phenomenon. *Arab J. Geosci.* 6, 3293–3302. doi:10.1007/s12517-012-0612-8

Kijko, A., Smit, A., and Sellevoll, M. A. (2016). Estimation of Earthquake Hazard Parameters from Incomplete Data Files. Part III. Incorporation of Uncertainty of Earthquake-Occurrence Model. *Bull. Seismological Soc. America* 106, 1210–1222. doi:10.1785/0120150252

Kim, H.-h., and Kyung, J. B. (2015). Analysis on the Relationship between Intensity and Magnitude for Historical Earthquakes in the Korean Peninsula. *J. Korean Earth Sci. Soc.* 36, 643–648. doi:10.5467/jkess.2015.36.7.643

Kim, H.-J., Jou, H.-T., Cho, H.-M., Bijwaard, H., Sato, T., Hong, J.-K., et al. (2003). Crustal Structure of the continental Margin of Korea in the East Sea (Japan Sea) from Deep Seismic Sounding Data: Evidence for Rifting Affected by the Hotter Than normal Mantle. *Tectonophysics* 364, 25–42. doi:10.1016/s0040-1951(03)00048-9

Kim, H.-J., Jou, H.-T., and Lee, G. H. (2018). Neotectonics of the Eastern Korean Margin Inferred from Back-Arc Rifting Structure. *Ocean Sci. J.* 53, 601–609. doi:10.1007/s12601-018-0036-9

Kim, H.-J., Lee, G. H., Choi, D.-L., Jou, H.-T., Li, Z., Zheng, Y., et al. (2015). Back-arc Rifting in the Korea Plateau in the East Sea (Japan Sea) and the Separation of the Southwestern Japan Arc from the Korean Margin. *Tectonophysics* 638, 147–157. doi:10.1016/j.tecto.2014.11.003

Kim, H.-J., Lee, G. H., Jou, H.-T., Cho, H.-M., Yoo, H.-S., Park, G.-T., et al. (2007). Evolution of the Eastern Margin of Korea: Constraints on the Opening of the East Sea (Japan Sea). *Tectonophysics* 436, 37–55. doi:10.1016/j.tecto.2007.02.014

Korea Meteorological Administration (2012). *Historical Earthquake Records in Korea*. Seoul: Korea Meteorological Administration, 279pp.

Lee, G. H., Yoon, Y., Nam, B. H., Lim, H., Kim, Y.-S., Kim, H. J., et al. (2011). Structural Evolution of the Southwestern Margin of the Ulleung Basin, East Sea (Japan Sea) and Tectonic Implications. *Tectonophysics* 502, 293–307. doi:10.1016/j.tecto.2011.01.015

Lister, G. S., Etheridge, M. A., and Symonds, P. A. (1986). Detachment Faulting and the Evolution of Passive continental Margins. *Geol* 14, 246–250. doi:10.1130/0091-7613(1986)14<246:dfateo>2.0.co;2

McCann, T., and Saintot, A. (2003). Tracing Tectonic Deformation Using the Sedimentary Record: an Overview. *Geol. Soc. Lond. Spec. Publications* 208, 1–28. doi:10.1144/gsl.sp.2003.208.01.01

McClay, K. R. (1990). Extensional Fault Systems in Sedimentary Basins: a Review of Analogue Model Studies. *Mar. Pet. Geology.* 7, 206–233. doi:10.1016/0264-8172(90)90001-w

Menegon, L., Campbell, L., Mancktelow, N., Camacho, A., Wex, S., Papa, S., et al. (2021). The Earthquake Cycle in the Dry Lower continental Crust: Insights from Two Deeply Exhumed Terranes (Musgrave Ranges, Australia and Lofoten, Norway). *Phil. Trans. R. Soc. A.* 379, 20190416. doi:10.1098/rsta.2019.04110.1098/rsta.2019.0416

Noh, M. H., Lee, S. K., and Choi, K. R. (2000). Minimum Magnitude of Earthquake Catalog of Korea Meteorological Agency for the Estimation of Seismicity Parameters. *J. Korean Geophys. Soc.* 3, 261–268.

Rhie, J., and Kim, S. (2010). Regional Moment Tensor Determination in the Southern Korean Peninsula. *Geosci. J.* 14, 329–333. doi:10.1007/s12303-010-0038-9

Rosendahl, B. R., Reynolds, D. J., Lorber, P. M., Burgess, C. F., McGill, J., Scott, D., et al. (1986). "Structural Expressions of Rifting: Lessons from Lake Tanganyika, Africa,".*Geol. Soc. Spec. Publ. Sedimentation in the African Rifts*. Editor L. E. Frostick (Boston, Blackwell Scientific Publications), 25, 29–43. doi:10.1144/gsl.sp.1986.025.01.04

Sheen, D.-H. (2015). Comparison of Local Magnitude Scales in South Korea. *Journal of the geological society of Korea* 51, 415–424. doi:10.14770/jgsk.2015.51.4.415

Tsoy, I. B., Gorovaya, M. T., Vasilenko, L. N., Vashchenkova, N. G., and Vagina, N. K. (2017). Age and Conditions of Formation of Sedimentary Cover of the Ulleung Plateau of the Sea of Japan According to Micropaleontological Data. *Stratigr. Geol. Correl.* 25, 99–121. doi:10.1134/s0869593817010063

Wu, Y.-M., Chen, S. K., Huang, T.-C., Huang, H.-H., Chao, W.-A., and Koulakov, I. (2018). Relationship Between Earthquake B -Values and Crustal Stresses in a Young Orogenic Belt. *Geophys. Res. Lett.* 45, 1832–1837. doi:10.1002/2017GL076694

Conflict of Interest: The authors declare that the research was conducted in the absence of any commercial or financial relationships that could be construed as a potential conflict of interest.